Catalysis Today 176 (2011) 277–280

Contents lists available at ScienceDirect

Catalysis Today

journal homepage: www.elsevier.com/locate/cattod

Formaldehyde total oxidation over mesoporous MnO_x catalysts

Jhon Quiroz Torres, Jean-Marc Giraudon, Jean-François Lamonier*

Université de Lille 1, Unité de Catalyse et Chimie du Solide, UMR CNRS 8181, 59652 Villeneuve d'Ascq, France

ARTICLE INFO

Article history:
Received 1 October 2010
Received in revised form
26 November 2010
Accepted 30 November 2010
Available online 6 January 2011

Keywords:
VOC
Oxidation
Formaldehyde
Manganese oxides

ABSTRACT

Manganese oxide mesoporous materials were prepared by using the template assisted method followed by an acidic treatment and tested in the formaldehyde oxidation. The structural, textural and redox properties of MnO_x samples were deeply modified when an acidic treatment was carried out after the calcination step: (i) Mn_3O_4 was transformed to Mn_5O_8 phase, (ii) the surface specific area was increased in 75%, and (iii) the redox properties were promoted at low temperature due to the oxidation of Mn^{3+} into Mn^{4+}. As a result, the catalytic oxidation of formaldehyde took place at lower temperatures. When cetyltrimethylammonium bromide surfactant was employed during the preparation, a narrow pore sire distribution was observed after the acidic treatment, leading to a material with high HCOH capacity adsorption and catalytic performance.

1. Introduction

Formaldehyde (HCOH) is regarded as the major indoor air pollutant emitted from widely used building and decorative materials. Long-term exposure to indoor air containing even few ppb of HCOH may cause adverse effects on human health [1]. Catalytic oxidation is one of the most promising technologies for controlling HCOH pollutant. For instance, noble metals supported catalysts have been reported to possess high activity for the complete oxidation of hundreds ppm of HCOH into CO_2 and H_2O [2]. However, the concentration of indoor HCOH emission is much lower (<1 ppm) and the corresponding catalytic treatment is more energy consuming at this condition. Consequently, for this application it is crucial to develop a material combining high capacity adsorption and catalytic performances. Mixed-valent octahedral molecular sieves (OMS) of manganese oxides, which can have applications in energy storage, as acid catalysts and in ion-exchange processes, are extensively reported. The generation of mixed-valent manganese oxide materials might lead to versatile systems for oxidation catalysis, such as VOC oxidation, CO and hydrocarbon oxidation [3].

It is well-known that the preparation method can influence the properties of catalyst. Recently, a new method involving surfactant in the precipitation process has been used [4,5]. The obtained catalyst shows high surface area and enhanced catalytic activities. Sinha et al. [6] have synthesized manganese oxide mesoporous material by using cetyltrimethylammonium bromide (CTAB) as template. This mesoporous oxide material shows high specific surface area and wormhole-like mesoporous structure showing advantage in contrast to those prepared by other methods, since this material is able to eliminate hexane and toluene at room temperature. Beley and Brenet [7] have demonstrated that by acidic treatment it is possible to obtain manganese oxide with higher oxidation states. This could be interesting for catalytic oxidation reaction. Thus, in this work we present the preparation of mesoporous manganese oxide catalysts using the surfactant assisted wet-chemistry route followed by acidic treatment. The techniques of X-ray diffraction (XRD), X-ray photoelectron spectroscopy (XPS), nitrogen adsorption–desorption isotherms and temperature-programmed reduction (H_2-TPR) were employed for catalyst characterization. Application of these materials to low-temperature formaldehyde elimination is also discussed.

2. Experimental

2.1. Catalyst preparation

Manganese oxides were prepared by precipitation from aqueous solution of nitrate involving the cetyltrimethylammonium bromide surfactant in the process. In a specific synthesis 16.7 g of $Mn(NO_3)_2{\cdot}6H_2O$ were dissolved in 150 mL of H_2O followed by the addition of a solution of NaOH (4.8 g NaOH in 50 mL of H_2O). The solution with the resulting manganese hydroxide precipitate was added to an aqueous solution of cetyltrimethylammonium bromide (67 g in 150 mL of H_2O dissolved at 30 °C). The resulting mixture was heated to 75 °C and then stirred for 1 h. The final gel obtained in a sealed beaker was transferred to an oven and heated for 12 h

---

* Corresponding author.
E-mail address: jean-francois.lamonier@univ-lille1.fr (J.-F. Lamonier).

0920-5861/$ – see front matter © 2010 Elsevier B.V. All rights reserved.
doi:10.1016/j.cattod.2010.11.089

at 75 °C. The solid residue was filtered, washed with water, dried in air and finally calcined at 500 °C for 6 h (1 °C min^{-1}). The calcined sample was treated with an aqueous solution of H_2SO_4 (120 mL to 10 mol L^{-1}) by stirring in a beaker for 1 h. The final product was filtered, and the residue was washed with water and dried at 105 °C. The obtained solids were denoted MnSC and MnSC_AT, calcined and acid treated respectively.

For comparison manganese oxides have been also prepared without surfactant using the same procedure as above. The resulting samples were denoted MnWSC and MnWSC_AT.

2.2. Catalyst characterization

Powder X-ray diffraction (XRD) patterns were recorded on a Bruker X-ray diffractometer at room temperature with Cu Kα radiation (λ = 1.5418 Å). The data of 2θ in the 5–80° range were collected with a step size of 0.02°. The diffraction patterns have been indexed by comparison with the Joint Committee on Powder Diffraction Standards (JCPDS) files. Nitrogen adsorption/desorption isotherms were obtained at −196 °C on a Micromeritics ASAP 2010 apparatus. The BET and BJH analyses were used to determine the total specific surface area, pore volume and pore size distribution of the samples. The XPS analyses were performed using a Kratos Analytical AXIS Ultra^{DLD} spectrometer. A monochromatized aluminium source (Al Kα = 1486.6 eV) was used for excitation. The C 1s (285.0 eV) binding energy (BE) was used as internal reference. Temperature-programmed reduction (H_2-TPR) measurements were performed on a Micromeritics AutoChem apparatus, 50 mg of the sample was heated from room temperature to 800 °C using a gas mixture of H_2 (5 vol.%)–Ar.

2.3. Catalytic activity test

The formaldehyde catalytic oxidation was performed in a fixed bed reactor (i.d. 10 mm) loaded with 200 mg of the catalyst. The reaction mixture containing 500 ppm HCOH, 20 vol.% O_2 was balanced by He. The effluent gas from the reactor containing formaldehyde, oxygen, carbon dioxide and carbon monoxide was analyzed by Varian MicroGC chromatograph equipped with thermal conductivity detector.

3. Results and discussion

3.1. Bulk structure and specific surface area

The wide angle powder XRD patterns of the MnO_x solids calcined and treated with sulphuric acid, are displayed in Fig. 1. For the calcined MnWSC and MnSC samples the main peaks of the patterns are those of the hausmanite phase Mn_3O_4 (JCPDS 07-1841). Additionally some peaks of lower intensities ascribed to monoclinic phase Mn_5O_8 (JCPDS 39-1218) are also detected. For the calcined MnSC solid using surfactant the diffraction profile show also the crystallization of bixbyite Mn_2O_3 (JCPDS 07-0856). The oxidative atmosphere used at the beginning of the synthesis provides a pathway to oxidize some Mn^{2+} present in $Mn(OH)_2$ to Mn^{3+} and Mn^{4+}. During the calcination step, the Mn^{3+} ions of the Mn_3O_4 are partially oxidized into Mn^{4+} ions to give Mn_5O_8 $(Mn_2{}^{2+}Mn_3{}^{4+})O_8{}^{-2}$ but a higher proportion of this phase seems to be produced when surfactant is employed (Fig. 1). This is probably due to the generation of hot spot by carbon based template exothermic decomposition which can enhance the transformation of Mn_3O_4 into Mn_5O_8. The existence of Mn_2O_3 in MnSC sample is related to the phase transformation of Mn_5O_8 in which the divalent and tetravalent Mn ions synproportionate to yield Mn_2O_3 [8]. After acidic treatment, the peaks due to the hausmanite and bixbyite phase disappear and only peaks due to the monoclinic phase Mn_5O_8 are observed. Beley and Brenet [7] showed that Mn^{2+} and Mn^{3+} can be transformed in the presence of sulphuric acid according to the following dismutation reaction:

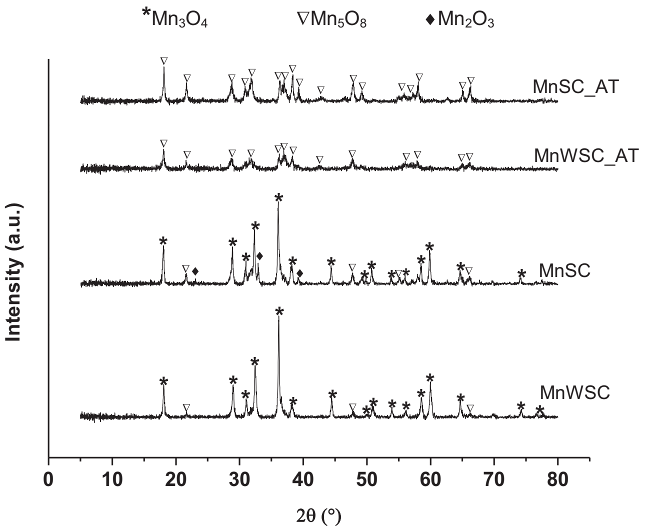

Fig. 1. XRD patterns of the calcined and acid treated MnO_x samples.

$$Mn_3O_4 + 4H^+ \rightarrow MnO_2 + 2Mn^{2+} + 2H_2O$$

In accordance with this reaction, the phase resulting from complete transformation of Mn_3O_4 in the presence of sulphuric acid should be MnO_2, although the monoclinic phase Mn_5O_8 is obtained in our experiments. Then it seems that a partial amount of Mn^{3+} can be oxidized leading to Mn_5O_8 monoclinic phase, which stabilizes the divalent Mn ions inherited from Mn_3O_4. Digestion time and acid concentration could explain this discrepancy [7].

The texture properties of the samples are listed in Table 1. For the calcined samples the specific surface area (SSA) are similar, indicating that the use of surfactant does not significantly modify their textural properties. However, the acidic treatment has spectacular effect on the SSA of the samples (increase of 75%), this effect being equivalent for both samples. This increase in the SSA is probably related to the decrease of the particle size under the strong acidic conditions. This assumption is supported by wide angle XRD results, which showed weaker and broader peaks of Mn_5O_8 monoclinic phase and then smaller crystallite size after the acidic treatment (Fig. 1). Sinha et al. [6] showed that the strong acidic condition breaks down larger particles into smaller ones significantly increasing the SSA. Fig. 2 shows the pore size distribution

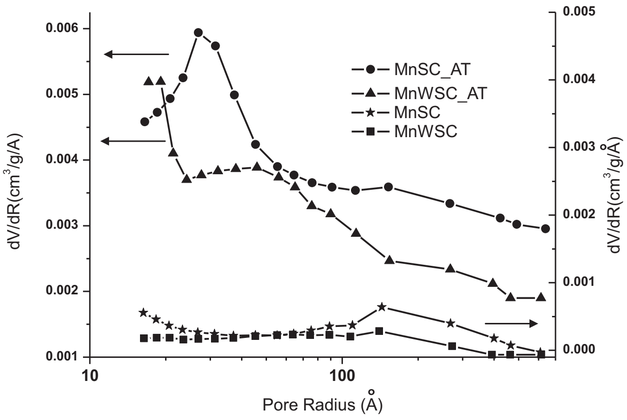

Fig. 2. Pore size distribution of the calcined and acid treated MnO_x samples.

Table 1
Characterization results of the calcined and acid treated MnO_x samples.

Sample	BET (m^2/g)	BJH desorption average pore radius (Å)	Consumed H_2 (mmol/g)	Average oxidation state[a]	Mn 3s ΔE (eV)
MnWSC	31	89	5.2	2.8	5.5
MnSC	20	91	6.3	3.0	5.4
MnWSC_AT	121	70	7.6	3.2	4.9
MnSC_AT	90	53	8.6	3.4	4.9

[a] From TPR results.

of the samples before and after the acidic treatment. For the calcined samples, a broad pore size distribution is observed with a similar value of average pore radius (Table 1), result consistent with the SSA value (Fig. 2). For the MnSC_AT sample, a narrow mesoporous distribution centered at 3 nm is observed, whereas for the sample MnWSC_AT these narrow mesopores are not present. This result could be explained by the presence of some ordered mesopores in the MnSC sample. After the acidic treatment of this sample, the breakdown of the particles seems to create narrow mesoporous distribution (Fig. 2) and smaller average pore radius (Table 1).

3.2. Redox properties

Fig. 3 shows the H_2-TPR profiles of the calcined and acid treated MnO_x materials. The reduction profiles are characterized by two regions of hydrogen consumption extended in the ranges 150–400 °C (LTR) and 400–650 °C (HTR). Several authors have obtained these profiles in MnO_x solids and in general it has been established that the LTR could be assigned to the reduction of poorly crystalline MnO_2/Mn_2O_3 into Mn_3O_4, while the HTR would correspond to the reduction Mn_3O_4 to MnO [9–12]. For the calcined and acid treated samples prepared using surfactant template, the peaks of the LTR and HTR are shifted towards lower temperatures, this shift being more pronounced on the calcined samples than on the acid treated samples. The H_2-TPR profiles of the acid treated samples show a higher contribution of LTR towards the total reduction profile, indicating that manganese ions are probably present in higher oxidation state. This result is in agreement with that obtained by XRD diffraction, in which the oxidation of the Mn_3O_4 during the acidic treatment generates Mn_5O_8 monoclinic phase with manganese ions in higher oxidation states. As a consequence the total H_2 consumption increases when the acidic treatment is carried out (Table 1). The average oxidation states (AOS) from TPR analyses are shown in Table 1. These values were estimated from the following equation:

$$Mn^{y+} + \frac{y-2}{2}H_2 = Mn^{2+} + (y-2)H^+$$

where y^+ is the AOS of Mn ions. AOS values of 2.8 and 3 were obtained for the calcined MnWSC and MnSC samples, respectively (Table 1). This result could be also correlated to the presence of Mn_5O_8 phase in higher proportion in the MnSC sample (Fig. 1). After acidic treatment, an increase in the AOS values is observed, according to the presence of Mn^{4+} in higher proportion.

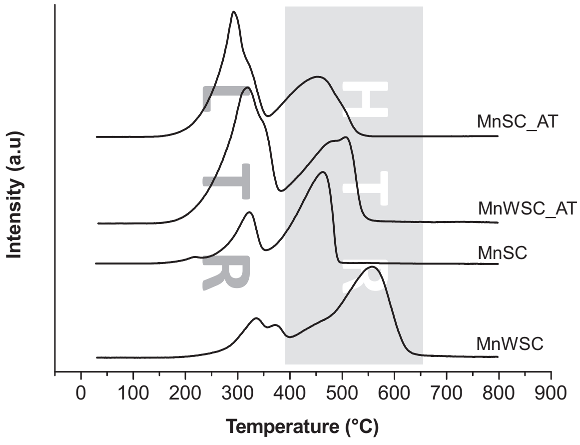

Fig. 3. H_2-TPR profiles of the calcined and acid treated MnO_x samples.

3.3. XPS analyses

The oxidation state of catalyst surface species was examined by XPS. The binding energy of the Mn $2p_{3/2}$ component of various Mn ions is very close to each other and a distinct identification is not possible [13,14]. However, the Mn(3s) peak splitting widths for different manganese oxides are helpful to find out the oxidation states [15–18]. The oxidation states of the samples are identified through direct comparison to standard values in the literature related to the Mn(3s) peak splitting width ΔE. Table 1 shows the values of ΔE for the calcined and acid treated samples. The calcined samples show a Mn(3s) ΔE of 5.5 eV, which corresponds to a mixed valence of +2 and +3. This result is in agreement with Mn_3O_4 phase identified by XRD. After acidic treatment, differences were observed in the Mn(3s) peak splitting widths. For both samples the value of $\Delta E = 4.9$ eV provides evidence of the presence of Mn^{4+} species. It may be reminded that these samples showed X-ray diffractions peaks corresponding to Mn_5O_8 and a higher AOS deduced from TPR analysis.

3.4. Catalytic activity test

Fig. 4 shows the variation in the concentration of HCOH and CO_2 during the catalytic test for the synthesized materials. No CO is detected during the HCOH oxidation, indicating the good selectivity of the samples to produce only CO_2 and H_2O. In the presence of MnWSC and MnWSC_AT catalysts, the HCOH is fully transformed at 200 °C and 160 °C respectively. This improvement in the catalytic activity can be explained by the redox properties enhancement (Fig. 3). Indeed it is generally postulated that VOC catalytic oxidation on metal oxides takes place via a redox mechanism in which the rate determining step would be the oxygen removal of the metal oxide used for VOC oxidation [19]. Therefore, the catalytic behaviour observed in the formaldehyde oxidation is well correlated to the easiest reduction observed by H_2-TPR for the acid treated samples. HCOH complete conversion is reached at 165 °C and 145 °C for the MnSC and MnSC_AT catalysts, respectively. This result shows that the use of surfactant during the preparation allowed to obtain MnO_x solids with higher catalytic activity. Additionally, it must be noted an increase in HCOH concentration at low temperature for the acid treated samples. This result could be explained by the HCOH desorption from MnWSC_AT and MnSC_AT catalysts upon temperature increase. Further studies are in progress to evaluate the quantity of adsorbed formaldehyde

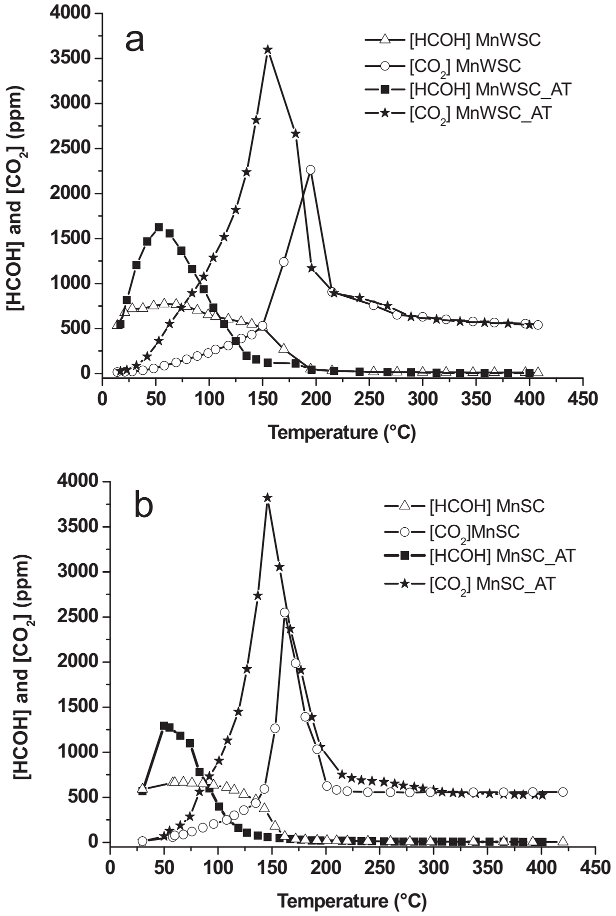

Fig. 4. Variation of HCOH and CO_2 concentration with the reaction temperature over the calcined and acid treated MnO_x catalysts synthesized (a) without surfactant and (b) with surfactant.

at room temperature. This result is in line with the spectacular enhancement of their specific surface areas after acidic treatment (Table 1). The CO_2 concentration gradually increases at low temperature and then reaches the maximum concentration at HCOH complete conversion. It seems also to be correlated to the HCOH and CO_2 adsorption capacity of the solids.

4. Conclusion

Mesoporous manganese oxide materials were synthesized by the surfactant assisted wet-chemistry route followed by acidic treatment. The acidic treatment had important effect in the SSA (increase of 75%), redox properties and manganese oxidation state (bulk and surface). High formaldehyde removal ability and capacity adsorption at low temperature were observed in the presence of acid treated MnO_x samples. The catalytic performance in HCOH oxidation was emphasized when the cetyltrimethylammonium bromide surfactant was used for the preparation of MnO_x samples before the acidic treatment. The formation of narrow mesopores and manganese species in high oxidation state in MnO_x sample seems to be responsible for this catalytic property enhancement.

Acknowledgements

Jhon Quiroz Torres thanks FUNDAYACUCHO (Caracas, Vanezuela) and French Embassy for the fellowship awarded. The authors thank the European Community and the Region “Nord Pas de Calais” for financial supports through Interreg IV “Redugaz” and IRENI projects.

References

[1] Y. Sekine, Atmos. Environ. 36 (2008) 5543.
[2] C. Zhang, H. He, K. Tanaka, Catal. Commun. 6 (2005) 211.
[3] Z. Tian, W. Tong, J. Wang, N. Duan, V. Krishnan, S. Suib, Science 276 (1997) 926.
[4] M. Luo, J. Ma, J. Lu, Y. Song, Y. Wang, J. Catal. 246 (2007) 52.
[5] J. Cao, Y. Wang, T. Zhang, S. Wu, Z. Yuan, Appl. Catal. B: Environ. 78 (2008) 120.
[6] A. Sinha, K. Suzuki, M. Takahara, H. Azuma, T. Nonaka, N. Suzuki, N. Takahashi, J. Phys. Chem. C 112 (2008) 16028.
[7] M. Beley, J. Brenet, Electrochim. Acta 18 (1973) 1003.
[8] B. Gillot, M. El Guendouzi, M. Laarj, Mater. Chem. Phys. 70 (2001) 54.
[9] F. Kapteijn, L. Singoredjo, A. Andreini, Appl. Catal. B: Environ. 3 (1994) 173.
[10] F. Arena, T. Torre, C. Raimondo, A. Parmaliana, Phys. Chem. Chem. Phys. 3 (2001) 1911.
[11] H. Chen, A. Sayari, A. Adnot, F. Larachi, Appl. Catal. B: Environ. 32 (2001) 195.
[12] F. Arena, G. Trunfio, J. Negro, B. Fazio, L. Spaparo, Chem. Mater. 19 (2007) 2269.
[13] R. Dula, R. Janik, T. Machej, J. Stoch, R. Grabowsky, E. Serwicka, Catal. Today 119 (2007) 327.
[14] T. Rao, M. Shen, L. Jia, J. Hao, J. Wang, Catal. Commun. 8 (2007) 1743.
[15] B. Djurfors, J. Broughton, M. Brett, D. Ivey, Acta Mater. 53 (2005) 957.
[16] M. Chigane, M. Ishikawa, J. Electrochem. Soc. 147 (2000) 2246.
[17] J. Carver, G. Schweitzer, T. Carlson, J. Chem. Phys. 57 (1972) 973.
[18] B. Murugan, A. Ramaswamy, Chem. Mater. 17 (2005) 3983.
[19] J. Spivey, Ind. Eng. Chem. Res. 26 (1987) 2165.